Inorganic Chemistry

ARTICLE

pubs.acs.org/IC

Synthesis and Decarbonylation Reactions of the Triiron Phosphinidene Complex $[Fe_3Cp_3(\mu\text{-}H)(\mu_3\text{-}PPh)(CO)_4]$: Easy Cleavage and Formation of P−H and Fe−Fe Bonds

Celedonio M. Alvarez, M. Angeles Alvarez, M. Esther García, Rocío González, Alberto Ramos, and Miguel A. Ruiz*

Departamento de Química Orgánica e Inorgánica/IUQOEM, Universidad de Oviedo, E-33071 Oviedo, Spain

Supporting Information

ABSTRACT: The binuclear phosphine complex $[Fe_2Cp_2(\mu\text{-}CO)_2(CO)(PH_2Ph)]$ (Cp = η^5-C_5H_5) reacted with the acetonitrile adduct $[Fe_2Cp_2(\mu\text{-}CO)_2(CO)(NCMe)]$ in dichloromethane at 293 K to give the trinuclear hydride−phosphinidene derivative $[Fe_3Cp_3(\mu\text{-}H)(\mu_3\text{-}PPh)(CO)_4]$ as a mixture of cis,anti and trans isomers (Fe−Fe = 2.7217(6) Å for the cis,anti isomer). In contrast, photochemical treatment of the phosphine complex with $[Fe_2Cp_2(CO)_4]$ gave the phosphide-bridged complex *trans*-$[Fe_3Cp_3(\mu\text{-}PHPh)(\mu\text{-}CO)_2(CO)_3]$ as the major product, along with small amounts of the binuclear hydride−phosphide complexes $[Fe_2Cp_2(\mu\text{-}H)(\mu\text{-}PHPh)(CO)_2]$ (cis and trans isomers), which are more selectively prepared from $[Fe_2Cp_2(CO)_4]$ and PH_2Ph at 388 K. The photochemical decarbonylation of either of the mentioned triiron compounds led reversibly to three different products depending on the reaction conditions: (a) the 48-electron phosphinidene cluster $[Fe_3Cp_3(\mu\text{-}H)(\mu_3\text{-}PPh)(\mu\text{-}CO)_2]$ (Fe−Fe = 2.592(2)−2.718(2) Å); (b) the 50-electron complex $[Fe_3Cp_3(\mu\text{-}H)(\mu_3\text{-}PPh)(\mu\text{-}CO)(CO)_2]$, also having carbonyl- and hydride-bridged metal−metal bonds (Fe−Fe = 2.6177(3) and 2.7611(4) Å, respectively); and (c) the 48-electron phosphide cluster $[Fe_3Cp_3(\mu\text{-}PHPh)(\mu_3\text{-}CO)(\mu\text{-}CO)_2]$, an isomer of the latter phosphinidene complex now having three intermetallic bonds (Fe−Fe = 2.5332(8)−2.6158(8) Å).

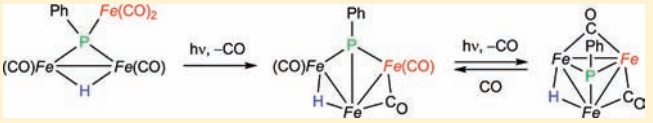

INTRODUCTION

We have recently shown that the phosphinidene complexes $[Fe_2Cp_2(\mu\text{-}PR)(\mu\text{-}CO)(CO)_2]$ (Cp = η^5-C_5H_5; R = Cy, Ph, 2,4,6-$C_6H_2Me_3$, 2,4,6-$C_6H_2{}^tBu_3$) can be readily prepared in high yields through a two-step procedure starting from the corresponding phosphine complexes $[Fe_2Cp_2(\mu\text{-}CO)_2(CO)(PH_2R)]$.[1] During the corresponding experimental studies we found that preparation of the phenylphosphine complex $[Fe_2Cp_2(\mu\text{-}CO)_2(CO)(PH_2Ph)]$ (**1**), which is made by reacting $[Fe_2Cp_2(\mu\text{-}CO)_2(CO)(NCMe)]$ with PH_2Ph in dichloromethane, occasionally yielded small amounts of a minor product. This product could be eventually isolated and fully identified as the hydride- and phosphinidene-bridged complex $[Fe_3Cp_3(\mu\text{-}H)(\mu_3\text{-}PPh)(CO)_4]$ (**2**, Chart 1). Formation of **2** is surprising if we consider the mild conditions under which this takes place (room temperature, dichloromethane solution), because two P−H bonds in the coordinated phosphine have to be cleaved along the way. Moreover, we noticed that because this 52-electron complex bears a $FeCp(CO)_2$ fragment, it should be therefore susceptible to decarbonylation to yield clusters with a phosphinidene ligand bridging three iron centers. Indeed, we have shown recently that related heterometallic species derived from the PCy complex $[Fe_2Cp_2(\mu\text{-}PCy)(\mu\text{-}CO)(CO)_2]$ can be decarbonylated photochemically, thus triggering formation of new metal−metal bonds to give new heterometallic clusters.[2] This synthetic strategy constitutes a new and rational approach to prepare μ_3-PR clusters to be added to other methods previously reported in the literature, often less selective.[2,3] Currently, the number of triiron phosphinidene complexes structurally characterized is rather limited,[4,5] even fewer of them also display bridging hydride ligands, and moreover none of them has cyclopentadienyl groups. We thus considered that compound **2** might be an interesting precursor for new triiron hydride phosphinidene complexes and clusters via its decarbonylation reactions.

In this paper we report our studies to develop an efficient synthetic route to the triiron phosphinidene complex **2** and a detailed analysis of its photochemical decarbonylation reactions. As it will be shown, this expectedly leads to reversible formation of new metal−metal bonds, but some unexpected processes are also observed, such as the photochemically induced reductive elimination of a P−H bond to yield a phosphide-bridged (instead of phosphinidene-bridged) product.

RESULTS AND DISCUSSION

Thermal and Photochemical Attempts To Prepare Compound 2. We have now found that although the phosphine complex **1** is itself prepared from the acetonitrile adduct $[Fe_2Cp_2(\mu\text{-}CO)_2(CO)(NCMe)]$ and PH_2Ph, it is still able to react slowly with a second molecule of this adduct at room temperature to give almost quantitatively the triiron phosphinidene derivative $[Fe_3Cp_3(\mu\text{-}H)(\mu_3\text{-}PPh)(CO)_4]$ (**2**). Inspection

Received: July 13, 2011
Published: October 07, 2011

dx.doi.org/10.1021/ic201491v | Inorg. Chem. 2011, 50, 10937–10948

Chart 1

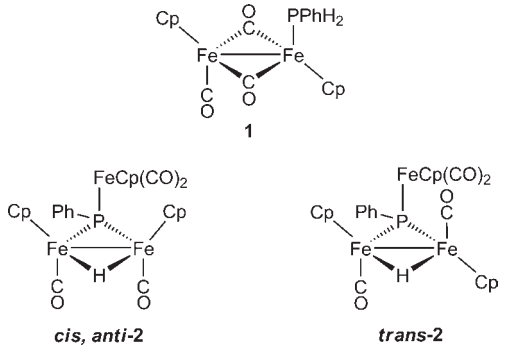

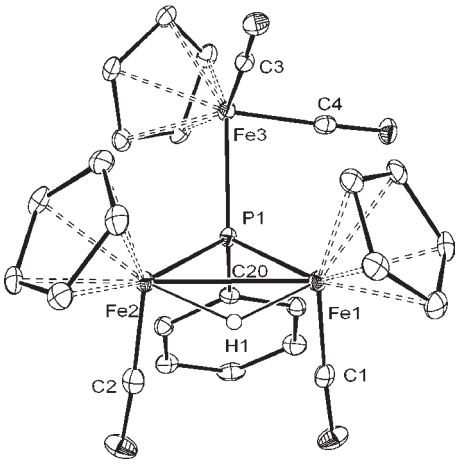

Figure 1. ORTEP diagram (30% probability) of compound *cis,anti*-**2** with H atoms (except the hydride ligand) omitted for clarity.

(by means of IR spectroscopy) of the reaction mixture allowed detection of significant amounts of the mononuclear hydride $[FeCpH(CO)_2]$, but this byproduct could not be isolated from the mixture, presumably because of its easy degradation to $[Fe_2Cp_2(CO)_4]$ during the workup.[6] Thus, formation of **2** seems to follow the stoichiometric balance implied by eq 1, as will be discussed later on.

$$[Fe_2Cp_2(\mu\text{-}CO)_2(CO)(PH_2Ph)](\mathbf{1}) + [Fe_2Cp_2(\mu\text{-}CO)_2(CO)(NCMe)] \rightarrow [FeCpH(CO)_2] + [Fe_3Cp_3(\mu\text{-}H)(\mu_3\text{-}PPh)(CO)_4](\mathbf{2}) + NCMe \quad (1)$$

We should note that there are three different isomers for complex **2** (Chart 1), depending on the relative arrangement of the FeCp(CO) fragments (cis and trans) and that of the latter Cp ligands with respect to the phenyl group on phosphorus (syn and anti). However, only two of these isomers are actually formed in the above reaction, these being identified as the cis,anti and trans isomers, with a relative ratio of ca. 11/2, according to the $^{31}P\{^1H\}$ NMR spectra of the crude reaction mixture. The third possible isomer (cis,syn) is not formed in this reaction, most likely because it would be the most disfavored one on steric grounds. We finally note that the cis and trans isomers of **2** do not interconvert in solution, even under irradiation with visible−UV light. This is in contrast with the behavior of the binuclear hydride−phosphide complex $[Fe_2Cp_2(\mu\text{-}H)(\mu\text{-}PPh_2)(CO)_2]$, which has been shown to undergo photochemically induced trans to cis isomerization.[7] In the case of **2**, decarbonylation takes place rapidly under these conditions instead, as it will be discussed below.

Table 1. Selected Bond Lengths (Å) and Angles (deg) for *cis, anti*-2

Fe1−Fe2	2.7217(6)	Fe1−P1−Fe2	75.7(1)
Fe1−P1	2.2181(8)	Fe1−P1−Fe3	124.1(1)
Fe2−P1	2.2174(8)	Fe2−P1−Fe3	124.4(1)
Fe3−P1	2.3363(8)	C1−Fe1−Fe2	95.5(1)
Fe1−C1	1.734(3)	C2−Fe2−Fe1	96.5(1)
Fe2−C2	1.740(3)	C3−Fe3−C4	95.0(1)
Fe3−C3	1.758(3)	C1−Fe1−P1	91.6(1)
Fe3−C4	1.765(3)	C2−Fe2−P1	95.7(1)
Fe1−H1	1.66(4)	C3−Fe3−P1	91.2(1)
Fe2−H1	1.68(4)	C4−Fe3−P1	87.9(1)
		H1−Fe1−P1	87(1)
		H1−Fe2−P1	86(1)

To obtain additional information on the elemental steps leading to **2**, we irradiated a mixture of $[Fe_2Cp_2(CO)_4]$ and **1** with visible−UV light in toluene at 288 K and using Pyrex glassware. Surprisingly, this only led to formation of small amounts of **2**. Instead, the major products were the binuclear hydride $[Fe_2Cp_2(\mu\text{-}H)(\mu\text{-}PHPh)(CO)_2]$ (**3a**) and the trinuclear complex *trans*-$[Fe_3Cp_3(\mu\text{-}PHPh)(\mu\text{-}CO)_2(CO)_3]$ (**4**). The hydride **3a** follows from decarbonylation of compound **1** (eq 2), and it can be more conveniently prepared from $[Fe_2Cp_2(CO)_4]$ and PH_2Ph. On the other hand, formation of compound **4** can be described through eq 3, and the elemental steps there involved will be discussed later on.

$$[Fe_2Cp_2(\mu\text{-}CO)_2(CO)(PH_2Ph)](\mathbf{1}) \rightarrow [Fe_2Cp_2(\mu\text{-}H)(\mu\text{-}PHPh)(CO)_2](\mathbf{3a}) + CO \quad (2)$$

$$[Fe_2Cp_2(\mu\text{-}CO)_2(CO)(PH_2Ph)](\mathbf{1}) + [Fe_2Cp_2(CO)_4] \rightarrow [FeCpH(CO)_2] + [Fe_3Cp_3(\mu\text{-}PHPh)(\mu\text{-}CO)_2(CO)_3](\mathbf{4}) \quad (3)$$

Structural Characterization of Compound 2. The structure of **2** was confirmed through a single-crystal study of the major cis, anti isomer (Figure 1 and Table 1). The molecule displays two FeCp(CO) fragments symmetrically bridged by hydride and PPh ligands (Fe−H ca. 1.67 Å and Fe−P ca. 2.22 Å), which define an almost flat Fe_2HP plane (angle between Fe_2H and Fe_2P planes ca. 15°), with the CO ligands placed almost parallel to each other and perpendicular to the intermetallic vector (Fe−Fe−C angles ca. 96°). The intermetallic distance of 2.7217(6) Å is consistent with the formulation of a single, H-bridged Fe−Fe bond, and it is comparable to the values of ca. 2.70 Å measured for the binuclear hydride−phosphide complexes $[Fe_2Cp_2(\mu\text{-}H)(\mu\text{-}PPh_2)(CO)_2]$[8] and $[Fe_2Cp_2(\mu\text{-}H)(\mu\text{-}PHMes)(CO)_2]$.[9] The phosphinidene ligand is also attached to a third metal fragment ($FeCp(CO)_2$), but the connection with this fragment is weaker, as deduced from the longer Fe3−P separation (2.3363(8) Å). This length is comparable to those measured in the trimetallaphosphonium cation $[\{FeCp(CO)_2\}_3(\mu_3\text{-}PH)]^+$ (ca. 2.33 Å)[10] and certainly longer than the values of ca. 2.13−2.21 Å

dx.doi.org/10.1021/ic201491v |*Inorg. Chem.* 2011, 50, 10937–10948

Table 2. Selected IR and NMR Data for New Compounds

compound	ν(CO)[a]	δ_P[b]	δ_H (J_{HP})[c]	
			μ-H	P−H
$[Fe_3Cp_3(\mu\text{-H})(\mu_3\text{-PPh})(CO)_4]$ (*trans*-**2**)	2010 (s), 1964 (s), 1918 (m, sh), 1905 (vs)[d]	246.1	−17.70 (33)	
$[Fe_3Cp_3(\mu\text{-H})(\mu_3\text{-PPh})(CO)_4]$ (*cis,anti*-**2**)	2005 (m), 1956 (s), 1938 (vs), 1899 (w)	258.7[e]	−18.51 (34)[e]	
$[Fe_2Cp_2(\mu\text{-H})(\mu\text{-PHPh})(CO)_2]$ (*trans*-**3a**)	1913	132.3[e,f]	−19.24 (43)[g]	6.00 (341)[g]
$[Fe_2Cp_2(\mu\text{-H})(\mu\text{-PHPh})(CO)_2]$ (*cis,anti*-**3a**)	1949 (vs), 1910 (w)	133.1[e]	−19.67 (43)[e]	5.26 (360)[e]
$[Fe_2Cp_2(\mu\text{-H})(\mu\text{-PHPh})(CO)_2]$ (*cis,syn*-**3a**)		137.6[e]	−20.25 (45)[e]	6.91 (321)[e]
$[Fe_2Cp_2(\mu\text{-H})(\mu\text{-PHCy})(CO)_2]$ (*trans*-**3b**)	1908	166.0	−19.15 (40)[e,g]	4.86 (316)[e,g]
$[Fe_2Cp_2(\mu\text{-H})(\mu\text{-PHCy})(CO)_2]$ (*cis*-**3b**)	1942 (vs), 1902 (w)	174.3	−20.23 (43)[e,g]	5.74 (300)[e,g]
$[Fe_3Cp_3(\mu\text{-PHPh})(\mu\text{-CO})_2(CO)_3]$ (**4**)	2023 (s), 1971 (s), 1924 (s), 1762 (w), 1721 (vs)	32.9		3.19 (298)
$[Fe_3Cp_3(\mu\text{-H})(\mu_3\text{-PPh})(\mu\text{-CO})(CO)_2]$ (*trans*-**5**)	1939 (m), 1921 (vs), 1787 (m)[d]	481.4	−26.37 (41)	
$[Fe_3Cp_3(\mu\text{-H})(\mu_3\text{-PPh})(\mu\text{-CO})(CO)_2]$ (*cis*-**5**)	1973 (vs), 1949 (m), 1787 (m)[d]	491.3	−25.63 (40)	
$[Fe_3Cp_3(\mu\text{-H})(\mu_3\text{-PPh})(\mu\text{-CO})_2]$ (**6**)	1769 (vs), 1727 (w)	506.5[f]	−34.82 (45)[g]	
$[Fe_3Cp_3(\mu\text{-PHPh})(\mu_3\text{-CO})(\mu\text{-CO})_2]$ (**7**)	1777 (vs), 1738 (m), 1644 (s)[d]	194.0[f]		6.66 (350)[g]

[a] Recorded in dichloromethane solution, with C−O stretching bands (ν(CO)) in cm^{-1}. [b] Recorded in CD_2Cl_2 solutions at 290 K and 121.52 MHz unless otherwise stated, with δ in ppm relative to external 85% aqueous H_3PO_4. [c] Recorded in CD_2Cl_2 solutions at 290 K and 300.13 MHz unless otherwise stated, with δ in ppm relative to internal $SiMe_4$ and P−H coupling constants (J_{HP}) in Hertz. [d] In toluene solution. [e] In $CDCl_3$ solution. [f] Recorded at 162.00 MHz. [g] Recorded at 400.13 MHz.

for different complexes of the type $[Fe_2Cp_2(\mu\text{-CO})_2(CO)(L)]$ having classical two-electron donor phosphines and phosphites (L)[7a,11] and hence dative P→Fe bonds. This is consistent with the prediction, based on simple electron counts, that the phosphinidene ligand in this molecule should formally provide the $Fe_2(\mu\text{-H})$ center with three electrons (PR_2-like coordination) and the $FeCp(CO)_2$ center with just one electron. This situation is comparable to that recently found by us in the photochemically generated complexes $[MFe_2Cp_2(\mu_3\text{-PCy})(\mu\text{-CO})(CO)_n]$ having an $MFe(\mu\text{-CO})$ core and a dangling $FeCp(CO)_2$ group (M = Cr, Fe)[2] and thus confirms a general trend in these complexes whereby M−P bonds to 17-electron metal fragments are significantly longer than M−P bonds to 16-electron metal fragments.

The spectroscopic data for the isomer *cis,anti*-**2** in solution are in good agreement with the solid-state structure just described (Table 2). Its IR spectrum in the C−O stretching region can be described as derived from the superimposition of the bands originated by relatively independent $FeCp(CO)_2$ and $Fe_2(CO)_2$ oscillators.[12] This allows assignment of the bands at 1938 (vs) and 1899 (w) cm^{-1} to the dimetal oscillator, with their relative intensities indicating an almost parallel arrangement of the $Fe_2(CO)_2$ carbonyls, as found in the crystal. The IR spectrum of *trans*-**2** can be interpreted along the same lines, but the relative intensities of the two less energetic bands (1918 (m, sh) and 1905 (vs) cm^{-1}) now clearly denote an antiparallel arrangement of carbonyls in the $Fe_2(CO)_2$ fragment (Chart 1).

The $^{31}P\{^1H\}$ NMR spectra of these compounds exhibit resonances at ca. 250 ppm, a position comparable to that of the photochemically generated compound $[Fe_3Cp_2(\mu_3\text{-PCy})(\mu\text{-CO})(CO)_6]$ having a dangling $FeCp(CO)_2$ group (283.7 ppm) but substantially shielded with respect to that of the isomer $[Fe_3Cp_2(\mu_3\text{-PCy})(\mu\text{-CO})(CO)_6]$ having a dangling $Fe(CO)_4$ group (421.5 ppm).[2] Thus, it seems that the chemical shift of the μ_3-PR ligand might be sensitive to the fine details of the electron distribution among the three metal atoms in these 52-electron complexes with just one metal−metal bond.

The different symmetry of the isomers of **2** is clearly reflected in their ^1H and ^{13}C NMR spectra. Thus, the asymmetric isomer trans gives rise to three different Cp and four different CO resonances. In contrast, the presence of a symmetry plane relating the FeCp(CO) fragments in the isomer cis,anti leads to the observation of just two sets of CO and Cp resonances. We finally note that the bridging hydride ligand in both isomers gives rise to a doublet resonance (J_{PH} ca. 33 Hz) at ca. −18 ppm, these being spectroscopic parameters comparable to those measured for compounds of the type $[Fe_2Cp_2(\mu\text{-H})(PRR')(CO)L]$ previously reported.[7]

Synthesis and Structural Characterization of Compounds 3. Although the hydride **3a** is obtained as a byproduct in the photochemical reaction between **1** and $[Fe_2Cp_2(CO)_4]$, it can be more conveniently prepared by reacting $[Fe_2Cp_2(CO)_4]$ and PH_2Ph in refluxing toluene. A similar reaction takes place with PH_2Cy to give the corresponding hydride derivative $[Fe_2Cp_2(\mu\text{-H})(\mu\text{-PHCy})(CO)_2]$ (**3b**) in high yield. This synthetic approach has been previously used by us and others to prepare related complexes of the type $[Fe_2Cp_2(\mu\text{-H})(\mu\text{-PR}_2)(CO)_2]$,[7,13] and we note that intermediates comparable to **1** were also detected by IR spectroscopy in the course of the formation of compounds **3**, suggesting the operation of a reaction pathway similar to that proposed for reaction of $[Fe_2Cp_2(CO)_4]$ with $PHPh_2$.[7]

As discussed for **2**, there are also three possible isomers for compounds **3**, depending on the relative disposition of the CO ligands (cis and trans) and that of the Cp groups with respect to the R substituent at the P atom (syn and anti). Actually all the possible isomers are formed for the phenyl compound **3a**, whereas only two of them could be detected for **3b**, these being the trans isomer and one of the cis isomers, which we assume it to be the cis,anti isomer, less disfavored on steric grounds (Chart 2). We note that the cis and trans isomers of these compounds do not interconvert in solution at room temperature and that they could be isolated separately in a conventional way. In contrast, the cis,syn and cis,anti isomers of **3a** could not be separated chromatographically, even if no interconversion between them seems to take place in solution either.

The IR spectra of compounds **3** in solution show a band at ca. 1910 cm^{-1} for the trans isomers and two bands at ca. 1945 (vs)

dx.doi.org/10.1021/ic201491v |*Inorg. Chem.* 2011, 50, 10937–10948

Chart 2

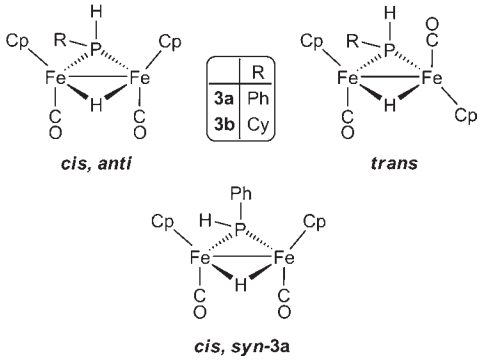

Chart 3

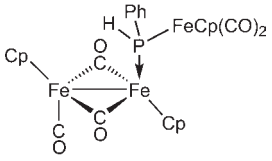

and 1905 (w) cm^{-1} for the cis isomers, as expected for this type of $M_2(CO)_2$ oscillators.[12] The trans isomers are also identified by the chemical inequivalence of their Cp ligands, and they give rise to ^{31}P NMR resonances, at 132.3 (**3a**) and 166.0 (**3b**) ppm, comparable to those measured for related PHR-bridged complexes.[13] The cis isomers have equivalent Cp groups and give rise to ^{31}P resonances slightly more deshielded. We finally note that, as expected for molecules having a $Fe_2(\mu\text{-H})(\mu\text{-PHR})$ central core, all these isomers display strongly coupled H−P resonances (δ_H ca. 5−7 ppm, with $^1J_{PH}$ ca. 300−360 Hz) and highly shielded hydride resonances (ca. −20 ppm, with $^2J_{PH}$ ca. 43 Hz).

Structural Characterization of Compound 4. The structure proposed for **4** can be derived from that of **1** by just replacing one of the P-bound H atoms with a $FeCp(CO)_2$ group, so that the terminal phosphine ligand in **1** becomes a bridging phosphide group in **4** (Chart 3). Since there is no metal−metal bond connecting the corresponding iron atoms, it is expected that the P atom becomes considerably shielded,[14] and this is consistent with the very low chemical shift of the complex (δ_P 32.9 ppm). The IR spectrum of **4** can be interpreted considering relatively independent oscillators: the two bands at lower frequencies are not very different from the corresponding bands in **1** and are assigned to the C−O stretches of a flat $M_2(\mu\text{-CO})_2$ oscillator, as denoted by their relative intensities; the two strong bands at higher frequencies are comparable to the corresponding bands in **2** and therefore can be attributed to the $FeCp(CO)_2$ moiety; finally, the band at 1924 cm^{-1} must necessarily correspond to the C−O stretch of the FeCp(CO) fragment, and its relatively low frequency must be taken as an indication of a transoid arrangement of the P and CO ligands around the central $Fe_2(\mu\text{-CO})_2$ core.[7,15]

Reaction Pathways in Formation of Compounds 2 and 4. As discussed above, compound **2** is obtained almost quantitatively by reacting **1** with the adduct $[Fe_2Cp_2(\mu\text{-CO})_2(CO)(NCMe)]$ in dichloromethane at room temperature. The latter complex is

Scheme 1. Possible Pathway for Formation of 2

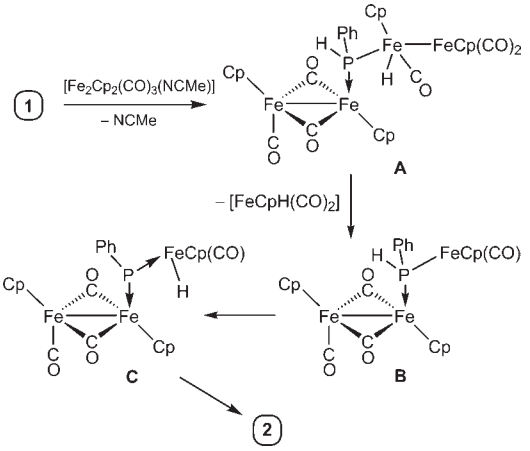

known to decompose progressively at the same temperature and solvent to give the tetracarbonyl $[Fe_2Cp_2(CO)_4]$ as the only carbonylic product. Therefore, we might guess that, to some extent, this adduct undergoes acetonitrile dissociation even in the absence of a good donor to give unstable intermediates of formula $[Fe_2Cp_2(CO)_3]$. The latter species are actually known (if unstable) transient species that can be photochemically generated from $[Fe_2Cp_2(CO)_4]$,[16,17] and they have been experimentally shown to undergo oxidative addition of the H−Sn bond of $HSnBu_3$ to eventually give a mixture of $[FeCp(CO)_2H]$ and $[FeCp(CO)_2(SnBu_3)]$.[18] In the same line, we propose that compound **1** would easily add to the $[Fe_2Cp_2(CO)_3]$ intermediate resulting from acetonitrile dissociation, this triggering the oxidative addition of one of the P−H bonds of the coordinated phosphine, to give the hydride−phosphide intermediate **A** (Scheme 1). Actually, this is not very different from the mechanism proposed previously for formation of $[Fe_2Cp_2(\mu\text{-H})(\mu\text{-PPh}_2)(CO)_2]$ upon decarbonylation of $[Fe_2Cp_2(\mu\text{-CO})_2(CO)(PHPh_2)]$.[7b] Intermediate **A** would then rapidly degrade by releasing $[FeCpH(CO)_2]$ (observed spectroscopically), this leaving a trimetallic intermediate **B** having a 16-electron center that would trigger a second oxidative addition of the remaining P−H bond to give the hydride−phosphinidene intermediate **C**, eventually yielding **2** after some rearrangement. The transformation of a μ-PHR ligand into a hydride−phosphinidene derivative is a rare event, but we can quote at least a few examples taking place at Os_3[19] or FeCoRu[20] centers to give μ_3-PR derivatives. More recently, we have shown that two metal centers are enough to promote this transformation under mild conditions if electronic and coordinative unsaturation are present, as proved by the formation at room temperature of the cation $[Mo_2Cp_2(\mu\text{-H})(\mu\text{-PR})(CO)_4]^+$ upon proton-induced dehydrogenation of $[Mo_2Cp_2(\mu\text{-H})(\mu\text{-PHR})(CO)_4]$, when R is the bulky substituent 2,4,6-$C_6H_2{}^tBu_3$.[21]

As stated above, photolysis of $[Fe_2Cp_2(CO)_4]$ in the presence of **1** led only to formation of small amounts of **2**, while the major products were the binuclear hydride complex **3a** and the trinuclear pentacarbonyl **4**. The hydride **3a** obviously follows from the photochemically induced decarbonylation of **1**, a process not very different from the thermal formation of this complex (vide supra). To explain the formation of **4** we must take into account that photolysis of $[Fe_2Cp_2(CO)_4]$ actually generates large amounts of the 17-electron radical $[FeCp(CO)_2]$ following

dx.doi.org/10.1021/ic201491v |*Inorg. Chem.* 2011, 50, 10937–10948

Scheme 2. Possible Pathway for the Formation of 4

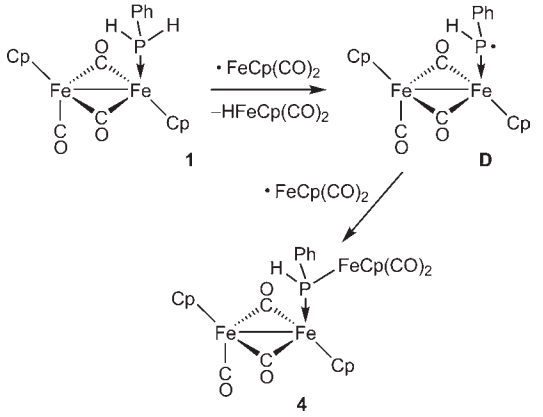

Chart 4

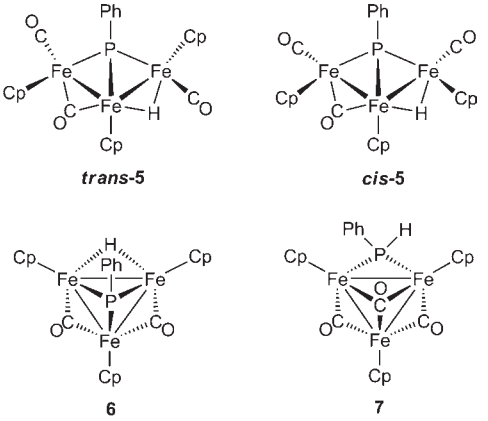

Scheme 3. Photolytic Reactions of Compounds 2 and 4

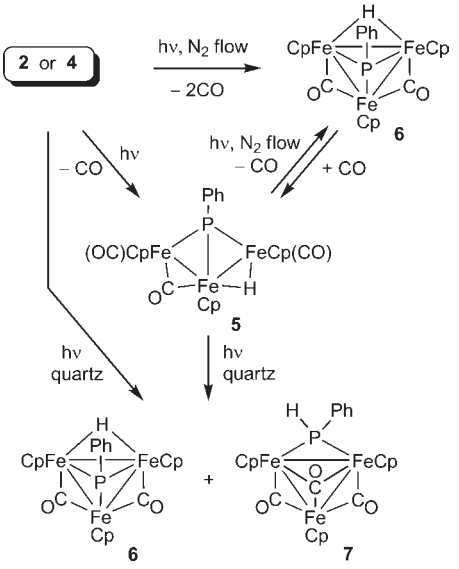

homolysis of the Fe−Fe bond, a process competing with the CO dissociation pathways leading to tricarbonyl intermediates $[Fe_2Cp_2(CO)_3]$.[16−18] Then we might conceive that the iron radical would initiate cleavage of a H−P bond by an atom transfer mechanism. This is a well-documented reaction of 17-electron organometallic complexes ML_n toward different X−Y bonds that can lead to both X−ML_n and Y−ML_n derivatives.[18,22] In our case, the corresponding derivatives would be $[FeCpH(CO)_2]$ and **4**, and a radical intermediate **D** would be involved (Scheme 2). However, we must note here that we found no examples of related reactions involving the P−H bond of a coordinated phosphine.

Photochemical Decarbonylation of Compounds 2 and 4. Removal of CO from **2** or **4** could be accomplished photochemically, triggering stepwise and reversible formation of new Fe−Fe bonds to yield different clusters depending on the precise experimental conditions (Scheme 3). Thus, irradiation of toluene solutions of the tetracarbonyl **2** with visible−UV light at 288 K and using Pyrex glassware gave the tricarbonyl derivative $[Fe_3Cp_3(\mu\text{-H})(\mu_3\text{-PPh})(\mu\text{-CO})(CO)_2]$ (**5**) in quantitative yields. This compound exists in solution as an equilibrium mixture of the corresponding cis and trans isomers (Chart 4) with their ratio being ca. 1/10 in C_6D_6 and 1/5 in CD_2Cl_2. If, however, a flow of N_2 is gently bubbled through solution under the same conditions (to facilitate removal of CO) then the reaction does not stop at the tricarbonyl step but proceeds with evolution of a second molecule of CO to eventually give the dicarbonyl cluster $[Fe_3Cp_3(\mu\text{-H})(\mu_3\text{-PPh})(\mu\text{-CO})_2]$ (**6**) after 2 h. The same result is achieved (but in shorter reaction times) if quartz glassware is used in the latter reaction, and a separate experiment confirmed that **5** is quantitatively transformed into **6** under any of the above photolytic conditions. The latter process is reversible, and compound **5** can be regenerated in 30 min by reaction of **6** with CO (1 atm) in toluene at 293 K. We finally note that the same results, and in comparable reaction times, were obtained in the above photolytic experiments when using the pentacarbonyl **4** instead of the tetracarbonyl **2**, although no detectable amounts of **2** were identified spectroscopically in the course of the corresponding reactions. This indicates that compounds **2** and **4** are decarbonylated to give **5** through independent reaction pathways, a matter to be discussed later on.

Photolysis at 288 K of either **2** or **5** using quartz glassware and without the N_2 purge leads to an inseparable 2/1 mixture of the dicarbonyl **6** and the tricarbonyl phosphide-bridged cluster $[Fe_3Cp_3(\mu\text{-PHPh})(\mu_3\text{-CO})(\mu\text{-CO})_2]$ (**7**). Fortunately, the new complex was inert toward CO, and the **6** + **7** mixture could be converted into a mixture of **5** and **7** by reaction with CO, allowing isolation of the latter. We note that photolysis of the pentacarbonyl **4** using quartz glassware and no N_2 purge also yielded a mixture of compounds **6** and **7** in 30 min at 288 K. Since **5** and **7** are isomeric species, we also attempted to obtain selectively **7** from **5** with no success. For instance, irradiation of **5** using quartz glassware and a CO atmosphere (to prevent formation of **6**) led to no neat transformation after 3 h. Likewise, no transformation of **5** could be detected in refluxing toluene after 1 h.

Structural Characterization of Compound 5. The structure of the trans isomer of **5** is built from three metal fragments bridged by a phosphinidene ligand and defining a V-shaped metal core (Figure 2 and Table 3). The external FeCp(CO) groups are arranged in a mutually transoid disposition, and the central FeCp moiety is connected to the other two by intermetallic bonds with carbonyl and hydride bridges over them, the latter being positioned opposite the PPh ligand, with respect to the intermetallic

dx.doi.org/10.1021/ic201491v |*Inorg. Chem.* 2011, 50, 10937–10948

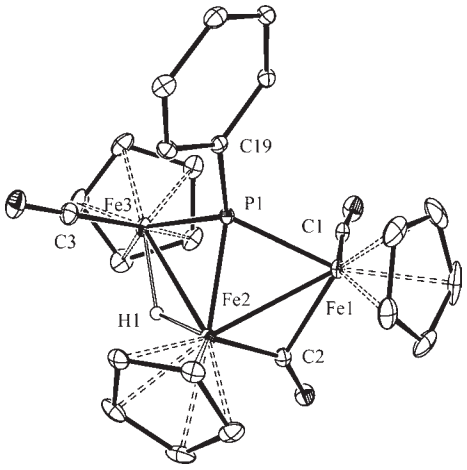

Figure 2. ORTEP diagram (30% probability) of *trans*-**5** with H atoms (except the hydride ligand) omitted for clarity.

Table 3. Selected Bond Lengths (Å) and Angles (deg) for *trans*-5

Fe1−Fe2	2.6177(3)	Fe1−Fe2−Fe3	89.9(1)
Fe2−Fe3	2.7611(4)	Fe1−P1−Fe2	73.8(1)
Fe1−P1	2.2010(5)	Fe1−P1−Fe3	120.5(1)
Fe2−P1	2.1593(5)	Fe2−P1−Fe3	79.1(7)
Fe3−P1	2.1787(5)	Fe1−P1−C19	116.1(1)
Fe1−C1	1.739(2)	Fe2−P1−C19	129.6(1)
Fe1−C2	2.079(2)	Fe3−P1−C19	122.1(1)
Fe2−C2	1.840(2)	C1−Fe1−P1	92.6(1)
Fe3−C3	1.749(2)	C2−Fe1−P1	88.5(1)
Fe2−H1	1.66(3)	C2−Fe2−P1	96.3(1)
Fe3−H1	1.61(3)	C3−Fe3−P1	91.9(1)

plane. The respective Fe−Fe lengths of 2.6177(3) and 2.7611(4) Å are within the range of values previously measured for related 48- and 50-electron $Fe_3(\mu_3\text{-PR})$ clusters,[4,5] with the tricentric $Fe_2(\mu\text{-H})$ bond being expectedly longer. The observed difference in the Fe−Fe lengths of **5** (ca. 0.15 Å) is, however, larger than anticipated (cf. 0.03 Å for $[Fe_3(\mu\text{-H})_2(\mu_3\text{-PPh})(CO)_9]$[4a] or $[Fe_3(\mu\text{-H})(\mu\text{-PMe}^i\text{Pr})(\mu_3\text{-PPh})(CO)_9]$,[23] with the latter being the only other 50-electron triiron hydride phosphinidene complex structurally characterized previously). In the case of **5**, the large difference in the Fe−Fe lengths might be attributed to the favorable combination of two opposite effects: a lengthening in one bond, due to the presence of the hydride ligand, and a contraction on the other bond, due to the presence of the bridging carbonyl. The phosphinidene ligand in **5** displays comparable and short Fe−P lengths (ca. 2.16−2.20 Å), with an environment around P quite distorted from the tetrahedral geometry, with the P, C19, Fe1, and Fe3 atoms almost in the same plane (Σ X−P−Y ca. 359°; X, Y = C19, Fe1, Fe3). This environment seems to be characteristic of 50-electron $Fe_3(\mu_3\text{-PR})$ and related clusters.[5,3]

Although the trans and cis isomers of **5** can be separated by chromatographic techniques, they quickly isomerize (ca. 10 min at 293 K) to reach a solvent-dependent equilibrium. The IR spectra of the mixture of isomers in the terminal C−O stretching region allow us to identify the relative disposition of the FeCp(CO) in these molecules: the major isomer gives bands at 1939 (m) and 1921 (vs) cm^{-1} and is therefore identified as the trans isomer, while these relative intensities are reversed in the minor species (1973 (vs) and 1949 (m) cm^{-1}), which is then identified as the cis isomer.[12] Both isomers give rise to strongly deshielded ^{31}P NMR resonances (ca. 490 ppm), some 240 ppm above that of **2**, and to strongly shielded resonances for the bridging hydride (at ca. −26 ppm, with J_{HP} ca. 40 Hz), in agreement with the retention of the bridging coordination of these ligands in solution.

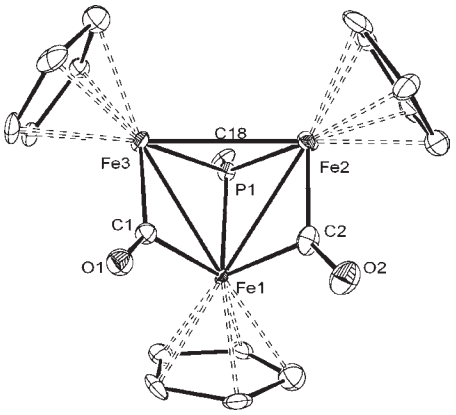

Figure 3. ORTEP diagram (30% probability) for one of the molecules in the asymmetric unit of **6**, with H atoms and the Ph group (except the C^1 atom) omitted for clarity.

Table 4. Selected Bond Lengths (Å) and Angles (deg) for 6

Fe1−Fe2	2.629(2)	Fe1−Fe2−Fe3	57.9(1)
Fe1−Fe3	2.591(2)	Fe1−Fe3−Fe2	59.3(1)
Fe2−Fe3	2.718(2)	Fe2−Fe1−Fe3	62.8(1)
Fe1−P1	2.144(3)	C1−Fe1−C2	79.4(4)
Fe2−P1	2.100(3)	Fe1−P1−Fe2	76.5(1)
Fe3−P1	2.122(3)	Fe1−P1−Fe3	74.8(1)
Fe1−C1	1.99(1)	Fe2−P1−Fe3	80.2(1)
Fe1−C2	1.97(1)	C1−Fe1−P1	98.2(3)
Fe2−C2	1.87(1)	C1−Fe3−P1	102.3(4)
Fe3−C1	1.89(1)	C2−Fe1−P1	96.0(4)
		C2−Fe2−P1	100.8(3)

Structural Characterization of Compound 6. Although the quality of our diffraction data for **6** was not optimal and the hydride ligand could not be located, all other structural features of the molecule are well defined (Figure 3 and Table 4). The cluster is built from three FeCp fragments defining a triangle bridged by a μ_3-PPh ligand displaying quite short P−Fe lengths (ca. 2.10−2.14 Å). The shortest Fe−Fe bonds (ca. 2.60 Å) are bridged by a carbonyl ligand each, and the third edge of the triangle is significantly longer (2.718(2) Å), presumably because of the presence of the bridging hydride over that edge. That intermetallic separation is now comparable to the corresponding ones in the isoelectronic complexes $[Fe_3(\mu\text{-H})_2(\mu_3\text{-PR})(CO)_9]$.[4a,c] As found for **5**, the bridging carbonyls are placed opposite the phosphinidene ligand, relative to the intermetallic plane, a feature also observed for the isoelectronic Fe_2Mn cluster $[Fe_2MnCp_2Cp'(\mu_3\text{-PCy})(\mu\text{-CO})_3]$ recently reported by us.[2]

The presence of a bridging hydride ligand in **6** is clearly denoted by the appearance of a strongly shielded resonance in its ^1H NMR spectrum (δ_H −35.82 ppm, J_{HP} = 45 Hz), while its IR spectrum in solution exhibits two C−O stretching bands in the

dx.doi.org/10.1021/ic201491v |*Inorg. Chem.* 2011, 50, 10937–10948

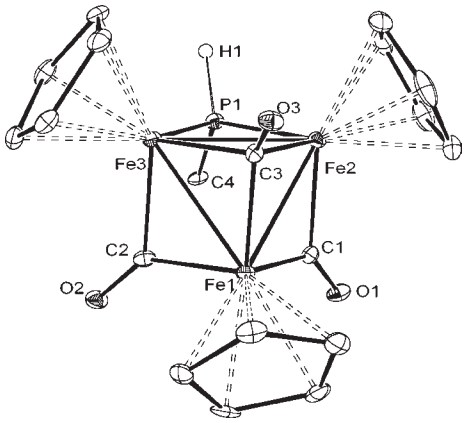

Figure 4. ORTEP diagram (30% probability) of compound **7** with H atoms (except the P−H) and Ph group (except the C^1 atom) omitted for clarity.

Table 5. Selected Bond Lengths (Å) and Angles (deg) for 7

Fe1−Fe2	2.5332(8)	Fe1−Fe2−Fe3	58.9(1)
Fe1−Fe3	2.5334(7)	Fe1−Fe3−Fe2	58.9(1)
Fe2−Fe3	2.6158(8)	Fe2−Fe1−Fe3	62.2(1)
Fe1−C1	1.914(4)	C1−Fe1−C3	100.6(2)
Fe1−C2	1.897(4)	C1−Fe2−C3	97.2(2)
Fe1−C3	1.937(4)	C2−Fe1−C3	100.6(2)
Fe2−C1	1.924(4)	C2−Fe3−C3	96.5(2)
Fe2−C3	2.022(4)	C3−Fe2−P1	101.6(1)
Fe3−C2	1.943(4)	C3−Fe3−P1	102.8(1)
Fe3−C3	2.009(4)	C2−Fe3−P1	86.8(1)
Fe2−P1	2.167(1)	C1−Fe2−P1	85.6(1)
Fe3−P1	2.147(1)	C1−Fe1−C2	89.7(2)
P1−H1	1.34(4)		

region of the bridging ligands, with relative intensities indicative of a cisoid arrangement, as found in the crystal. It should be noticed the progressive shielding of the μ_2-H ligand as we proceed from **2** (ca. −20 ppm) to **5** (ca. −25 ppm) and then to **6** (ca. −35 ppm). This hardly can be attributed to significant variations in the geometrical parameters within each $Fe_2(\mu$-H) unit. Instead, we trust that these shielding differences actually reflect the relative proximity of the third metal atom to the hydride ligand. In **2**, this metal center is too far away (ca. 4.74 Å) to cause a significant shielding on the hydride nucleus, hence the similitude of its chemical shift to those of the binuclear hydrides **3** (Table 2). In **5**, the third metal atom is significantly closer to the hydride ligand (3.51 Å), thus explaining the observed shielding of ca. 5 ppm relative to the former compounds. In **6**, it can be estimated that this distance is reduced to ca. 3.2 Å, thus explaining the large magnetic shielding of the hydride nucleus. We finally note that the phosphinidene ligand in **6** gives rise to a strongly deshielded ^{31}P NMR resonance (506.5 ppm). This shift is comparable to that of the 50 electron complex **5** but much higher than those observed for **2** and related heterometallic 52-electron PR-bridged complexes.[2]

Structural Characterization of Compound 7. This cluster is built from three FeCp fragments defining an isosceles triangle bridged by a μ_3-CO ligand (Figure 4 and Table 5). The shortest Fe−Fe edges (ca. 2.53 Å) are bridged by a carbonyl ligand each,

Scheme 4. Possible Pathway for the Formation of 5 from 2 [*Fe* = FeCp(CO)]

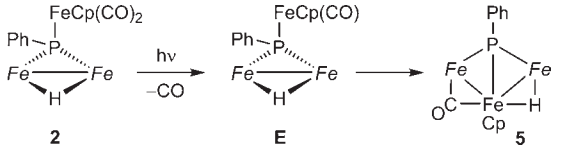

and the third edge of the triangle (ca. 2.62 Å) is bridged by a phenylphosphide ligand, with its Ph group pointing away from the intermetallic plane, presumably to minimize the steric repulsions with the Cp ligands. As found for **6**, the edge-bridging ligands are placed opposite the face-bridging ligand, relative to the intermetallic plane. The Fe−C bonds of that μ_3-CO ligand (av. 1.99 Å) are somewhat longer than those of the edge-bridging ones (av. 1.92 A) as expected, and have comparable lengths to those measured in the tetrahedral cluster $[Fe_4Cp_4(\mu_3\text{-CO})_4]$.[24] In the phosphinidene-bridged complex $[Fe_3(\mu_3\text{-P}^t\text{Bu})(\mu_3\text{-CO})(\text{CO})_6(\eta^6\text{-C}_6\text{H}_5\text{Me})]$ (a related molecule also having a 48-electron count) the Fe−CO lengths of the face-bridging ligand are much longer (ca. 2.21 Å),[25] a difference that can be attributed to the lower oxidation state of iron in that case.

The spectroscopic data in solution for **7** are consistent with the retention of its solid state structure. Its IR spectrum exhibits a band at very low frequency (1644 cm^{-1}) assigned to the C−O stretch of its face-bridging carbonyl, while the bands at 1777 (vs) and 1738 (m) cm^{-1} denote the presence of two edge-bridging carbonyls in a cisoid arrangement. These assignments were confirmed by the presence of resonances at 297.0 and 272.7 ppm (1:2 intensity) in the corresponding $^{13}C\{^1H\}$ NMR spectrum with the face-bridging carbonyl giving the most deshielded resonance as expected.[26] The $^{31}P\{^1H\}$ NMR spectrum of **7** exhibits a relatively shielded resonance (δ_P 194.0 ppm) with a shift comparable to that of the cation $[Fe_2Cp_2(\mu\text{-PPhH})(\mu\text{-CO})(\text{CO})_2]^+$,[1a,c] which is indicative of the retention of the PHPh ligand in solution, also denoted by the appearance of a strongly coupled PH resonance at 6.66 ppm ($^1J_{HP}$ = 350 Hz) in the ^{1}H NMR spectrum.

Reaction Pathways in Formation of Compounds 5−7. Formation of the tricarbonyl **5** from the tetracarbonyl **2** most likely involves loss of a terminal CO from the unique dicarbonyl fragment in the molecule ($FeCp(CO)_2$) to give the intermediate **E**, with a 16-electron FeCp(CO) center (Scheme 4). This would trigger formation of a new Fe−Fe bond with a simultaneous rearrangement of a terminal CO to a bridging position to give compound **5**. The process would be completely parallel to that recently proposed to explain formation of the isoelectronic complex $[Fe_2MnCp_2Cp'(\mu_3\text{-PCy})(\mu\text{-CO})_2(\text{CO})_2]$ from its 52-electron precursor $[Fe_2MnCp_2Cp'(\mu_3\text{-PCy})(\mu\text{-CO})(\text{CO})_4]$.[2]

In contrast, formation of **5** from **4** has to be more complex. It is sensible to assume that the reaction also involves first loss of a CO molecule from the unique $FeCp(CO)_2$ fragment of the complex (Scheme 5). This would give the same intermediate **B** that is presumably involved in thermal formation of **2** (Scheme 1). Since we have not detected the intermediacy of **2** in the way from **4** to **5**, we must assume that, under photolytic conditions, intermediate **B** does not decay thermally to **2** but instead undergoes a photochemical rearrangement, perhaps with formation of a new Fe−Fe bond to give a 50-electron intermediate **E** with a new $FeCp(CO)_2$ fragment. The photochemical decarbonylation of the latter fragment would now yield an

dx.doi.org/10.1021/ic201491v |*Inorg. Chem.* 2011, 50, 10937–10948

Scheme 5. Possible Pathway for Formation of 5 from 4

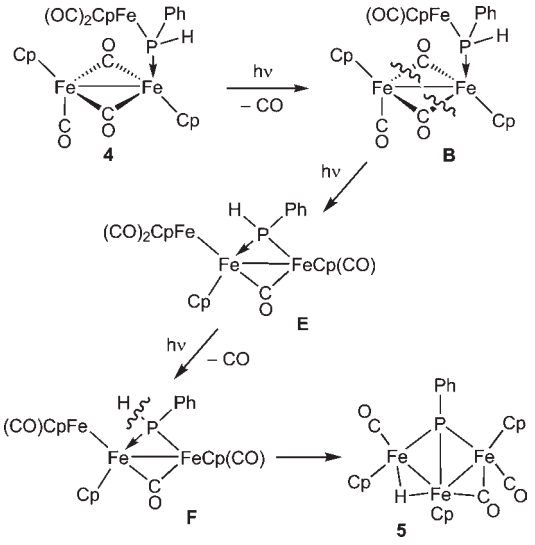

Scheme 6. Possible Pathway for Formation of Compounds 6 and 7 from 5 [*Fe* = FeCp]

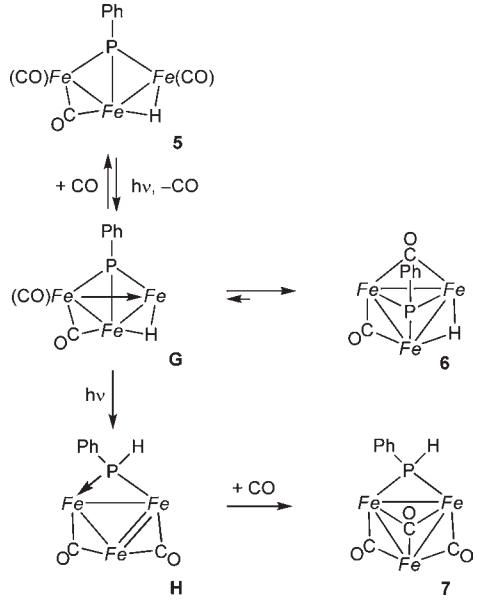

unsaturated intermediate **F** with a 16-electron FeCp(CO) center that would then trigger oxidative addition of the P−H bond of the phosphide ligand to finally give the phosphinidene **5**.

To explain formation of compounds **6** and **7**, we assume that decarbonylation of **5** should trigger formation of a new Fe−Fe bond, thus yielding a 48-electron intermediate **G**, rendering cluster **6** after a terminal to bridging rearrangement of the remaining carbonyl (Scheme 6). These two steps should be reversible, because **6** gives back **5** upon carbonylation. To account for formation of **7**, we must assume an alternative evolution of **G**, only operative under irradiation, via reductive elimination of μ-H and μ_3-PPh ligands to give an unsaturated μ_2-PHPh intermediate **H**, the latter reacting rapidly with CO to give the electron-precise cluster **7**. This proposal is fully consistent with the absence of **7** when a N_2 purge is used in the experiment (suppression of the **H**/**7** step) and the absence of **6** and **7** when photolysis is carried out under a CO atmosphere (suppression of the **5**/**G** step).

We should stress that the reductive formation of a P−H bond between μ-H and μ_3-PPh ligands leading to the PHPh-bridged cluster **7** is unexpected, especially under photolytic conditions (this usually would trigger the opposite process, as discussed in this work). Interestingly, we quote a couple of examples were reductive formation of a P−H bond is favored for a hydride−phosphinidene substrate, both of them involving anionic complexes containing *pyramidal* phosphinidene bridges (2-electron donors): this is the case of the cluster $[Os_3(\mu\text{-H})(\mu_2\text{-PPh})(CO)_{10}]^-$ [27] and the dimanganese anion $[Mn_2(\mu\text{-H})(\mu\text{-PCy})(CO)_8]^-$.[28]

CONCLUDING REMARKS

The room-temperature reaction of the phenylphosphine complex $[Fe_2Cp_2(\mu\text{-CO})_2(CO)(PH_2Ph)]$ with the acetonitrile adduct $[Fe_2Cp_2(\mu\text{-CO})_2(CO)(NCMe)]$ triggers spontaneous oxidative addition of two P−H bonds to eventually give the hydride−phosphinidene derivative $[Fe_3Cp_3(\mu\text{-H})(\mu_3\text{-PPh})(CO)_4]$ (**2**) in excellent yield, whereas its photochemical reaction with $[Fe_2Cp_2(CO)_4]$, using visible light, induces cleavage of a single P−H bond to give the phosphide derivative $[Fe_3Cp_3(\mu_3\text{-PHPh})(\mu\text{-CO})_2(CO)_3]$ (**4**). Photochemical decarbonylation of compounds **2** and **4** (using visible−UV light) can be tuned to give either 50-electron or 48-electron phosphinidene clusters having hydride ligands, following from stepwise formation of new Fe−Fe bonds. A phosphide-bridged cluster can be also formed under the right conditions, following from the unexpected reductive elimination of a P−H bond between hydride and μ_3-phosphinidene ligands.

EXPERIMENTAL SECTION

General Procedures and Starting Materials. All manipulations and reactions were carried out under a nitrogen (99.995%) atmosphere using standard Schlenk techniques. Solvents were purified according to literature procedures and distilled prior to use.[29] Petroleum ether refers to that fraction distilling in the range 338−343 K. Compounds **1**[1a,c] and $[Fe_2Cp_2(\mu\text{-CO})_2(CO)(NCMe)]$[30] were synthesized according to literature procedures. All other reagents were obtained from the usual commercial suppliers and used as received. Photochemical experiments were performed using jacketed quartz or Pyrex Schlenk tubes, cooled by tap water (ca. 288 K). A 400 W mercury lamp placed ca. 1 cm away from the Schlenk tube was used for the experiments with visible−UV light. Chromatographic separations were carried out using jacketed columns cooled by tap water (ca. 288 K) or by a closed 2-propanol circuit, kept at the desired temperature with a cryostat. Commercial aluminum oxide (activity I, 150 mesh) was degassed under vacuum prior to use. The latter was mixed under nitrogen with the appropriate amount of water to reach the activity desired. IR C−O stretching frequencies were measured in solution and are referred to as ν (CO). Nuclear magnetic resonance (NMR) spectra were routinely recorded at 300.13 (^{1}H), 121.52 (^{31}P{^{1}H}), and 75.48 MHz (^{13}C{^{1}H}) at 290 K in CD_2Cl_2 solutions unless otherwise stated. Chemical shifts (δ) are given in ppm, relative to internal tetramethylsilane (^{1}H, ^{13}C) or external 85% aqueous H_3PO_4 (^{31}P). Coupling constants (J) are given in Hertz.

*Preparation of [$Fe_3Cp_3(\mu$-H)(μ_3-PPh)(CO)$_4$] (**2**).* A dichloromethane solution (5 mL) of freshly prepared $[Fe_2Cp_2(\mu\text{-CO})_2(CO)(NCMe)]$ (ca. 2.260 mmol) was added to a dichloromethane solution (5 mL) of

compound **1** (0.500 g, 1.147 mmol), and the mixture was stirred for 16 h to give a red solution. The solvent was then removed under vacuum, and the residue was dissolved in a minimum amount of dichloromethane/petroleum ether (1/3) and chromatographed on alumina (activity II) at 288 K. Elution with the same solvent mixture gave a red fraction that gave, upon removal of solvents under vacuum, compound *trans*-**2** as an orange-reddish microcrystalline solid (0.067 g, 11%). Elution with dichloromethane/petroleum ether (1/2) gave a second red fraction giving analogously compound *cis,anti*-**2** as a red microcrystalline solid (0.569 g, 85%). X-ray-quality crystals of the latter compound were grown by slow diffusion of a layer of petroleum ether into a dichloromethane solution of the complex at 253 K. *Data for compound trans*-**2**. Anal. Calcd for $C_{25}H_{21}Fe_3O_4P$: C, 51.42; H, 3.62. Found: C, 51.29; H, 3.48. ^{1}H NMR: δ 7.91 (m, 2H, Ph), 7.25 (m, 2H, Ph), 7.15 (m, 1H, Ph), 4.67 (d, J_{HP} = 1, 5H, Cp), 4.64, 4.43 (2s, 2 × 5H, Cp), −17.70 (d, J_{HP} = 33, 1H, μ-H). ^{13}C{^{1}H} NMR: δ 218.6 (d, J_{CP} = 16, CO), 216.9 (d, J_{CP} = 17, CO), 215.8 (d, J_{CP} = 20, CO), 214.5 (d, J_{CP} = 14, CO), 158.1 [d, J_{CP} = 14, C^1−Ph], 132.4 (d, J_{CP} = 6, C^2−Ph), 126.9 (s, C^3−Ph), 126.8 (s, C^4−Ph), 88.1, 82.2, 81.9 (3s, Cp). *Data for compound cis,anti*-**2**. Anal. Calcd for $C_{25}H_{21}Fe_3O_4P$: C, 51.42; H, 3.62. Found: C, 51.26; H, 3.42. ^{1}H NMR ($CDCl_3$): δ 7.70 (m, 2H, Ph), 7.16 (m, 2H, Ph), 7.05 (m, 1H, Ph), 4.68 (s, 15H, Cp), −18.51 (d, J_{HP} = 34, 1H, μ-H). ^{13}C{^{1}H} NMR ($CDCl_3$): δ 215.8 (d, J_{CP} = 15, 2CO), 215.7 (d, J_{CP} = 16, 2CO), 156.3 (d, J_{CP} = 3, C^1−Ph), 131.5 (s, C^4−Ph), 126.5 (s, C^2 and C^3−Ph), 88.6 (s, Cp), 80.9 (s, 2Cp).

*Preparation of [$Fe_2Cp_2(\mu$-H)(μ-PHPh)(CO)$_2$] (**3a**).* A toluene solution (20 mL) containing [$Fe_2Cp_2(CO)_4$] (0.200 g, 0.565 mmol) and PH_2Ph (64 μL, 0.582 mmol) was refluxed for 2.5 h to give a red solution. The solvent was then removed under vacuum, and the solid residue thus obtained was dissolved in a minimum amount of dichloromethane/petroleum ether (1/8) and chromatographed on alumina (activity II) at 253 K. Elution with dichloromethane/petroleum ether (1/6) gave an orange fraction giving, after removal of solvents, compound *trans*-**3a** as an orange microcrystalline solid (0.160 g, 69%). Elution with dichloromethane/petroleum ether (1/4) gave another orange fraction yielding analogously compound *cis*-**3a** (0.048 g, 21%) as a mixture of the syn and anti isomers in a relative ratio of ca. 1/2. *Data for compound trans-**3a**.* Anal. Calcd for $C_{18}H_{17}Fe_2O_2P$: C, 52.99; H, 4.20. Found: C, 52.76; H, 4.16. ^{1}H NMR ($CDCl_3$): δ 7.78 (m, 2H, Ph), 7.47−7.27 (m, 3H, Ph), 6.00 (d, J_{HP} = 341, 1H, P−H), 4.57, 4.41 (2s, 2 × 5H, Cp), −19.24 (d, J_{HP} = 43, 1H, μ-H). *Data for compound cis-**3a**.* Anal. Calcd for $C_{18}H_{17}Fe_2O_2P$: C, 52.99; H, 4.20. Found: C, 52.68; H, 4.09. *Spectroscopic data for isomer cis,anti-**3a**.* ^{1}H NMR ($CDCl_3$): δ 7.68−7.25 (m, 5H, Ph), 5.26 (d, J_{HP} = 360, 1H, P−H), 4.54 (s, 10H, Cp), −19.67 (d, J_{HP} = 43, 1H, μ-H). *Spectroscopic data for isomer cis,syn-**3a**.* ^{1}H NMR ($CDCl_3$): δ 7.68−7.25 (m, 5H, Ph), 6.91 (d, J_{HP} = 321, 1H, P−H), 4.57 (s, 10H, Cp), −20.25 (d, J_{HP} = 45, 1H, μ-H).

*Preparation of [$Fe_2Cp_2(\mu$-H)(μ-PHCy)(CO)$_2$] (**3b**).* The procedure is completely analogous to that just described for **3a** but using PH_2Cy (76 μL, 0.572 mmol) and a reaction time of 3 h instead. In this way the compounds *trans*-**3b** (0.164 g, 70%) and *cis*-**3b** (0.040 g, 17%) were obtained as orange solids. *Data for compound trans-**3b**.* Anal. Calcd for $C_{18}H_{23}Fe_2O_2P$: C, 52.22; H, 5.60. Found: C, 52.12; H, 5.25. ^{1}H NMR (400.13 MHz, $CDCl_3$): δ 4.86 (ddd, J_{HP} = 316, J_{HH} = 9, 2, 1H, P−H), 4.55, 4.47 (2d, J_{HP} = 1, 2 × 5H, Cp), 2.45 (m, 1H, Cy), 2.32 (m, 1H, Cy), 1.95−1.27 (m, 9H, Cy), −19.15 (dd, J_{HP} = 40, J_{HH} = 2, 1H, μ-H). *Data for compound cis-**3b**.* Anal. Calcd for $C_{18}H_{23}Fe_2O_2P$: C, 52.22; H, 5.60. Found: C, 52.07; H, 5.39. ^{1}H NMR (400.13 MHz, $CDCl_3$): δ 5.74 (ddd, J_{HP} = 300, J_{HH} = 10, 1, 1H, P−H), 4.50 (d, J_{HP} = 1, 10H, Cp), 2.24−2.22 (m, 3H, Cy), 1.93−1.10 (m, 8H, Cy), −20.23 (dd, J_{HP} = 43, J_{HH} = 1, 1H, μ-H).

*Photochemical Reaction of Compound **1** with [$Fe_2Cp_2(CO)_4$].* A toluene solution (8 mL) containing compound **1** (0.100 g, 0.229 mmol) and [$Fe_2Cp_2(CO)_4$] (0.082 g, 0.232 mmol) was irradiated with visible−UV light for 1 h in a Pyrex Schlenk tube refrigerated with tap water while gently bubbling N_2 through the solution to give a brown-reddish solution. The solvent was then removed under vacuum, and the residue was dissolved in a minimum amount of dichloromethane/petroleum ether (1/2) and chromatographed on alumina (activity II) at 253 K. Elution with the same solvent mixture gave three different fractions: the first one gave, after removal of solvents, compound *trans*-**3a** as an orange solid (0.009 g, 10%), the second one, also orange, gave analogously compound *cis*-**3a** (0.023 g, 25%) as a mixture of the syn and anti isomers in a ratio 1/2, whereas the third one (red) contained some [$Fe_2Cp_2(CO)_4$]. Finally, elution with dichloromethane/petroleum ether (1/1) gave another red fraction yielding analogously compound *cis*-**2** (0.013 g, 10%) and then a green-purple fraction giving *trans*-[Fe_3Cp_3-(μ-PHPh)(μ-CO)$_2$(CO)$_3$] (**4**) as a purple solid (0.072 g, 52%). *Data for compound **4**.* Anal. Calcd for $C_{26}H_{21}Fe_3O_5P$: C, 51.03; H, 3.46. Found: C, 50.72; H, 3.18. ^{1}H NMR: δ 7.40−7.28 (m, 5H, Ph), 5.07 (d, J_{HP} = 2, 5H, Cp), 4.67 (s, 5H, Cp), 4.45 (d, J_{HP} = 2, 5H, Cp), 3.19 (d, J_{HP} = 298, 1H, P−H).

*Preparation of [$Fe_3Cp_3(\mu$-H)(μ_3-PPh)(μ-CO)(CO)$_2$] (**5**).* A toluene solution (4 mL) of compound *cis*-**2** (0.050 g, 0.086 mmol) was irradiated for 40 min with visible−UV light in a Pyrex Schlenk tube refrigerated with tap water while gently bubbling N_2 through the solution to give a brown mixture. The solvent was then removed under vacuum, and the residue was dissolved in a minimum amount of dichloromethane/petroleum ether (1/2) and chromatographed on alumina (activity IV) at 288 K. Elution with the same solvent mixture gave a green-brownish fraction containing *trans*-**5**, which isomerizes in solution outside the column to reach the equilibrium ratio with the corresponding isomer *cis*-**5** in ca. 10 min. Elution with dichloromethane/petroleum ether (1/1) gave a green fraction containing the isomer *cis*-**5**, which also isomerizes outside the column to reach the equilibrium ratio with the corresponding trans isomer. The fractions were mixed to give, after removal of solvents, compound **5** as a brown solid (0.039 g, 81%). The cis/trans equilibrium ratio in solution was measured (by NMR) to be ca. 1/10 in C_6D_6 and 1/5 in CD_2Cl_2. X-ray-quality crystals of *trans*-**5** were grown by slow diffusion of a layer of petroleum ether into a toluene solution of the mixture of isomers at 253 K. Using the same experimental procedure, irradiation of a toluene solution (5 mL) of *trans*-**2** (0.050 g, 0.086 mmol) for 30 min also gave compound **5** after similar workup (0.040 g, 84%). Anal. Calcd for $C_{24}H_{21}Fe_3O_3P$: C, 51.85; H, 3.81. Found: C, 51.69; H, 3.68. *Spectroscopic data for trans-**5**.* ^{1}H NMR: δ 8.44 (m, 2H, Ph), 7.75−7.57 (m, 3H, Ph), 4.57, 4.48, 4.36 (3s, 3 × 5H, Cp), −26.37 (d, J_{HP} = 41, 1H, μ-H). ^{1}H NMR (400.13 MHz, C_6D_6): δ 8.49 (m, 2H, Ph), 7.43 (m, 2H, Ph), 7.33 (m, 1H, Ph), 4.42, 4.25, 4.08 (3s, 3 × 5H, Cp), −26.05 (d, J_{HP} = 41, 1H, μ-H). ^{13}C{^{1}H} NMR (100.62 MHz): δ 260.5 (d, J_{CP} = 6, μ-CO), 219.3, 214.9 (2d, J_{CP} = 24, FeCO), 153.1 (d, J_{CP} = 11, C^1−Ph), 133.1 (d, J_{CP} = 8, C^2−Ph), 129.0 (s, C^4−Ph), 128.2 (d, J_{CP} = 9, C^3−Ph), 84.0, 83.9, 80.8 (3s, Cp). *Spectroscopic data for cis-**5**.* ^{1}H NMR: δ 8.38 (m, 2H, Ph), 7.72 (m, 2H, Ph), 7.17 (m, 1H, Ph), 4.69, 4.34, 4.21 (3s, 3 × 5H, Cp), −25.63 (d, J_{HP} = 40, 1H, μ-H). ^{1}H NMR (400.13 MHz, C_6D_6): δ 8.44 (m, 2H, Ph), 8.21 (m, 2H, Ph), 7.82 (m, 1H, Ph), 4.51, 3.98, 3.86 (3s, 3 × 5H, Cp), −25.51 (d, J_{HP} = 40, 1H, μ-H). ^{13}C{^{1}H} NMR (100.62 MHz): δ 263.2 (d, J_{CP} = 5, μ-CO), 216.3 (d, J_{CP} = 16, FeCO), 216.2 (d, J_{CP} = 17, FeCO), 154.7 (d, J_{CP} = 14, C^1−Ph), 131.3 (d, J_{CP} = 6, C^2−Ph), 128.7 (s, C^4−Ph), 128.6 (s, C^3−Ph), 84.4, 83.0, 81.7 (3s, Cp).

*Preparation of [$Fe_3Cp_3(\mu$-H)(μ_3-PPh)(μ-CO)$_2$] (**6**).* A toluene solution (10 mL) of *cis*-**2** (0.075 g, 0.128 mmol) was irradiated for 1 h with visible−UV light in a quartz Schlenk tube refrigerated with tap water while gently bubbling N_2 through the solution to give a red-brown solution. The solvent was then removed under vacuum, and the residue was dissolved in a minimum amount of dichloromethane/petroleum ether (1/2) and chromatographed on alumina (activity II) at 288 K. Elution with dichloromethane/petroleum ether (1/3) gave a brown-reddish fraction giving, upon removal of solvents, compound **6** as a brown microcrystalline

Table 6. Crystal Data for New Compounds

	2	5	6	7.
mol formula	$C_{25}H_{21}Fe_3O_4P$	$C_{24}H_{21}Fe_3O_3P$	$C_{23}H_{20}Fe_3O_2P$	$C_{24}H_{21}Fe_3O_3P$
mol wt	583.94	555.93	526.91	555.93
cryst syst	monoclinic	triclinic	orthorhombic	monoclinic
space group	$P2_1/c$	$P-1$	$Pna2_1$	$C2/c$
radiation (λ, Å)	0.71073	0.71073	0.71073	0.71073
a, Å	10.8336(3)	8.6127(3)	30.1320(8)	28.592(2)
b, Å	13.5644(4)	9.3554(3)	9.3911(2)	7.7225(5)
c, Å	16.2488(7)	14.2511(4)	14.1378(4)	18.428(1)
α, deg	90	78.704(2)	90	90
β, deg	109.481(1)	75.595(2)	90	91.669(2)
γ, deg	90	73.497(2)	90	90
V, Å^3	2251.1(1)	1056.63(6)	4000.6(2)	4067.3(5)
Z	4	2	8	8
calcd density, g cm^{-3}	1.723	1.747	1.750	1.816
absorp coeff, mm^{-1}	2.010	2.133	2.244	2.216
temperature, K	100(2)	100(2)	100(2)	100(2)
θ range (deg)	1.99−25.24	2.29−25.33	1.98−25.34	2.21−26.39
index ranges (h, k, l)	−12, 12; −16, 0; −19, 11	0, 10; −10, 11; −16, 17	−36, 0; 0, 11; −16, 17	−35, 35; 0, 9; 0, 23
no. of reflns collected	15 522	15 999	27 007	15 091
no. of indep reflns (R_{int})	3987 (0.0285)	3828 (0.0229)	7244 (0.0519)	4116 (0.0525)
reflns with $I > 2\sigma(I)$	3532	3640	6695	3044
R indexes [data with $I > 2\sigma(I)$][a]	$R_1 = 0.0311$, w$R_2 = 0.0847$[b]	$R_1 = 0.0218$, w$R_2 = 0.0553$[c]	$R_1 = 0.0861$, w$R_2 = 0.2122$[d]	$R_1 = 0.0397$, w$R_2 = 0.0821$[e]
R indexes (all data)[a]	$R_1 = 0.0375$, w$R_2 = 0.1032$[b]	$R_1 = 0.0232$, w$R_2 = 0.0561$[c]	$R_1 = 0.0953$, w$R_2 = 0.2237$[d]	$R_1 = 0.0685$, w$R_2 = 0.0935$[e]
GOF	1.186	1.114	1.093	1.047
no. of restraints/params	0/302	0/284	115/509	0/284
$\Delta\rho$(max, min), e Å^{-3}	0.634, −0.657	0.386, −0.286	5.655, −2.061	0.805, −0.617

[a] $R = \Sigma||F_o| - |F_c||/\Sigma|F_o|$. $wR = [\Sigma w(|F_o|^2 - |F_c|^2)^2/\Sigma w|F_o|^2]^{1/2}$. $w = 1/[\sigma^2(F_o^2) + (aP)^2 + bP]$, where $P = (F_o^2 + 2F_c^2)/3$. [b] $a = 0.0515$, $b = 2.4279$. [c] $a = 0.0246$, $b = 0.7989$. [d] $a = 0.1692$, $b = 11.2139$ [e] $a = 0.0337$, $b = 14.9859$.

solid (0.061 g, 90%). X-ray-quality crystals of **6** were grown by slow diffusion of layers of petroleum ether and toluene into a dichloromethane solution of the complex at 253 K. Anal. Calcd for $C_{23}H_{21}Fe_3O_2P$: C, 52.33; H, 4.01. Found: C, 52.18; H, 3.95. ^{1}H NMR (400.13 MHz): δ 8.85 (m, 2H, Ph), 7.90−7.82 (m, 3H, Ph), 4.28 (s, 10H, Cp), 4.14 (s, 5H, Cp), −34.82 (d, J_{HP} = 45, 1H, μ-H). ^{13}C{^{1}H} NMR (100.62 MHz): δ 273.8 (s, μ-CO), 145.3 (d, J_{CP} = 9, C^1−Ph), 134.5 (d, J_{CP} = 9, C^2−Ph), 131.9 (s, C^4−Ph), 129.6 (d, J_{CP} = 11, C^3−Ph), 86.5 (s, Cp), 81.2 (s, 2Cp).

*Preparation of [$Fe_3Cp_3(\mu$-PHPh)(μ_3-CO)(μ-CO)$_2$] (**7**).* A toluene solution (6 mL) of *cis*-**2** (0.060 g, 0.103 mmol) was irradiated for 2 h with visible−UV light in a quartz Schlenk tube refrigerated with tap water to give a brown solution. The mixture was then exposed to a CO atmosphere and further stirred for 10 min at room temperature to give a green solution. The solvent was then removed under vacuum, and the residue was dissolved in a minimum amount of dichloromethane/petroleum ether (1/1) and chromatographed on alumina (activity IV) at 288 K. Elution with dichloromethane/petroleum ether (1/2) gave a green-brownish fraction giving, upon removal of solvents, compound **5** (0.034 g, 59%). Elution with dichloromethane/petroleum ether (2/1) gave a dark-green fraction yielding analogously compound **7** as a green microcrystalline solid (0.020 g, 35%). X-ray-quality crystals of **7** were grown by slow diffusion of layers of petroleum ether and toluene into a dichloromethane solution of the compound at 253 K. Anal. Calcd for $C_{24}H_{21}Fe_3O_3P$: C, 51.85; H, 3.81. Found: C, 51.72; H, 3.77. ^{1}H NMR (400.13 MHz): δ 7.65 (m, 2H, Ph), 7.40 (m, 1H, Ph), 7.32 (m, 2H, Ph), 6.66 (d, J_{HP} = 350, 1H, P−H), 4.71 (d, J_{HP} = 1, 10H, Cp), 4.69 (s, 5H, Cp). ^{13}C{^{1}H} NMR (100.62 MHz): δ 297.0 (s, μ_3-CO), 272.7 (s, μ-CO), 147.6 (d, J_{CP} = 14, C^1−Ph), 134.3 (d, J_{CP} = 7, C^2−Ph), 130.0 (s, C^4−Ph), 128.3 (d, J_{CP} = 11, C^3−Ph), 94.3 (s, Cp), 90.3 (s, 2Cp).

*X-ray Structure Determination for Compounds **2**, **5**, and **6**.* The X-ray intensity data were collected at 100 K on a Nonius KappaCCD single-crystal diffractometer using graphite-monochromated Mo Kα radiation. Images were collected at a fixed crystal−detector distance (29 mm for **2**, 30 mm for **5**, and 45 mm for **6**) using the oscillation method with 1° (**2** and **5**) or 0.7° (**6**) oscillations and 40 s exposure time per image. Data collection strategies were calculated with the program Collect.[31] Data reduction and cell refinement were performed with the programs HKL Denzo and Scalepack.[32] A semiempirical absorption correction was applied using the program SORTAV.[33] Using the program suite WinGX,[34] the structures were solved by Patterson interpretation and phase expansion using SHELXL97[35] and refined with full-matrix least-squares on F^2 using SHELXL97. For compounds **2** and **5**, all non-hydrogen atoms were refined anisotropically and all hydrogen atoms were fixed at calculated positions except for the hydride H(1) atoms, which were located in the Fourier map and refined; all them were given an overall isotropic thermal parameter. For compound **6** two molecules of the complex were found to be present in the asymmetric unit. Moreover, due to the low quality of the diffraction data (some twinning was found to occur in the crystal but the twin law could not be determined), not all the positional parameters and anisotropic temperature factors of all the non-H atoms could be refined anisotropically. A significant number of atoms had to be refined anisotropically in combination with the instructions DELU and SIMU, and 3 atoms were finally refined isotropically to prevent their temperature factors from becoming nonpositive definite. Besides, restrictions in the C−C lengths

dx.doi.org/10.1021/ic201491v |*Inorg. Chem.* 2011, 50, 10937–10948

of the cyclopentadienyl rings had to be imposed for a convenient convergence. All hydrogen atoms were geometrically placed and refined using a riding model, except for the hydride ligand, which could not be located in the Fourier map nor modeled due to the low quality of the crystal. Crystallographic data and structure refinement details for compounds **2**, **5**, and **6** are collected in Table 6.

X-ray Structure Determination for Compound ***7***. X-ray intensity data were collected on a Kappa-Appex-II Bruker diffractometer using graphite-monochromated Mo Kα radiation at 100 K. The software APEX[36] was used for collecting frames with the ω/ϕ scans measurement method. The Bruker SAINT software was used for data reduction,[37] and a multiscan absorption correction was applied with SADABS.[38] Using the program suite WinGX,[34] the structure was solved by direct methods using SHELXL97[35] and refined with full-matrix least-squares on F^2 using SHELXL97. All positional parameters and anisotropic temperature factors of all the non-H atoms were refined anisotropically, and all hydrogen atoms were geometrically placed and refined using a riding model except for the P-bound H(1), which was located in the Fourier maps and refined isotropically. Crystallographic data and structure refinement details for **7** are collected in Table 6.

■ ASSOCIATED CONTENT

Ⓢ Supporting Information. CIF file giving crystallographic data for structural analysis of compounds **2**, **5**, **6**, and **7**. This material is available free of charge via the Internet at http://pubs.acs.org.

■ AUTHOR INFORMATION

Corresponding Author
*E-mail: mara@uniovi.es.

■ ACKNOWLEDGMENT

We thank the DGI of Spain (Projects CTQ2006-01207 and CTQ2009-09444) and the COST action CM0802 "PhoSciNet" for supporting this work and the MEC of Spain for a grant (to R.G.).

■ REFERENCES

(1) (a) Alvarez, C. M.; Alvarez, M. A.; García, M. E.; González, R.; Ruiz, M. A.; Hamidov, H.; Jeffery, J. C. *Organometallics* **2005**, *24*, 5503. (b) Alvarez, M. A.; García, M. E.; González, R.; Ramos, A.; Ruiz, M. A. *Organometallics* **2010**, *29*, 1875. (c) Alvarez, M. A.; García, M. E.; González, R.; Ramos, A.; Ruiz, M. A. *Organometallics* **2011**, *30*, 1102.

(2) Alvarez, M. A.; García, M. E.; González, R.; Ramos, A.; Ruiz, M. A. *Inorg. Chem.* **2011**, *50*, 7894.

(3) Huttner, G.; Knoll, K. *Angew. Chem., Int. Ed. Engl.* **1987**, *26*, 743.

(4) For representative 48-electron clusters see:(a) Huttner, G.; Schneider, J.; Mohr, G.; von Seyerl, J. *J. Organomet. Chem.* **1980**, *191*, 161. (b) Knoll, K.; Huttner, G.; Zsolnai, L.; Jibril, I.; Wasiucionek, M. *J. Organomet. Chem.* **1985**, *294*, 91. (c) Sunick, D. L.; White, P. S.; Schauer, C. K. *Organometallics* **1993**, *12*, 245. (d) Bitterer, F.; Kucken, S.; Langhans, K. P.; Stelzer, O.; Sheldrick, W. S. *Z. Naturforsh. B* **1994**, *49*, 1223. (e) Wang, D. Z.; Wu, W. F.; Liu, S. T.; Gong, P. J. *Chin. J. Inorg. Chem.* **2003**, *19*, 1090.

(5) For representative 50-electron complexes, see: (a) Winter, A.; Zsolnai, L.; Huttner, G. *J. Organomet. Chem.* **1982**, *234*, 337. (b) Cook, S. L.; Evans, J.; Gray, L. R.; Webster, M. *J. Organomet. Chem.* **1982**, *236*, 367. (c) Williams, G. D.; Geoffroy, G. L.; Whittle, R. R.; Rheingold, A. L. *J. Am. Chem. Soc.* **1985**, *107*, 729. (d) Sherer, O. J.; Gobel, K.; Kaub, J. *Angew. Chem., Int. Ed. Engl.* **1987**, *26*, 59. (e) Barlett, R. A.; Dias, H. V. R.; Flynn, K. M.; Olmstead, M. M.; Power, P. P. *J. Am. Chem. Soc.* **1987**, *109*, 5699. (f) Song, J. S.; Geoffroy, G. L.; Rheingold, A. L. *Inorg. Chem.* **1992**, *31*, 1505. (g) Bautista, M. T.; Jordan, M. R.; White, P. S.; Schauer, C. K. *Inorg. Chem.* **1993**, *32*, 5429. (h) Borg-Breen, C. C.; Bautista, M. T.; Schauer, C. K.; White, P. S. *J. Am. Chem. Soc.* **2000**, *122*, 3952.

(6) Shackleton, T. A.; Mackie, S, C.; Fergusson, S. B.; Johnston, L. J.; Baird, M. C. *Organometallics* **1990**, *9*, 2248.

(7) (a) Alvarez, C. M.; Galán, B.; García, M. E.; Riera, V.; Ruiz, M. A.; Vaissermann, J. *Organometallics* **2003**, *22*, 5504. (b) Alvarez, C. M.; García, M. E.; Ruiz, M. A.; Connelly, N. G. *Organometallics* **2004**, *23*, 4750.

(8) Decaen, A.; Craig, C. D.; Bottomley, F. *Acta Crystallogr., Sect. E* **2004**, *60*, 1284.

(9) Sugiura, J.; Kakizawa, T.; Hashimoto, H.; Tobita, H.; Ogino, H. *Organometallics* **2005**, *24*, 1099.

(10) Pohl, W.; Lorenz, I. P.; Noeth, H.; Schmidt, M. *Z. Naturforsch. B* **1995**, *50*, 1485.

(11) (a) Cotton, F. A.; Frenz, B. A.; White, A. J. *Inorg. Chem.* **1974**, *13*, 1407. (b) Klasen, C.; Lorenz, I. P.; Schmid, S.; Beuter, G. *J. Organomet. Chem.* **1992**, *428*, 363.

(12) Braterman, P. S. *Metal Carbonyl Spectra*; Academic Press: London, 1975.

(13) (a) Brunner, H.; Peter, H. *J. Organomet. Chem.* **1990**, *393*, 411. (b) Brunner, H.; Rötzer, M. *J. Organomet. Chem.* **1992**, *425*, 119.

(14) Carty, A. J.; MacLaughlin, S. A.; Nucciarone, D. In *Phosphorus-31 NMR Spectroscopy in Stereochemical Analysis*; Verkade, J. G., Quin, L. D., Eds.; VCH: Deerfield Beach, FL, 1987; Chapter 16.

(15) (a) Haines, R. J.; du Preez, A. L. *Inorg. Chem.* **1969**, *8*, 1459. (b) Klasen, C.; Lorenz, I. P.; Schmid, S.; Beuter, G. *J. Organomet. Chem.* **1992**, *428*, 363. (c) Zhang, S.; Brown, T. L. *Organometallics* **1992**, *11*, 4166.

(16) Bitterwolf, T. E. *Coord. Chem. Rev.* **2000**, *206*−*207*, 419.

(17) (a) Zhang, S.; Brown, T. L. *Organometallics* **1992**, *11*, 4166. (b) Zhang, S.; Brown, T. L. *J. Am. Chem. Soc.* **1993**, *113*, 1779.

(18) Zhang, S.; Brown, T. L. *Organometallics* **1992**, *11*, 2122.

(19) (a) Ebsworth, E. A. V.; McIntosh, A. P.; Schröder, M. *J. Organomet. Chem.* **1986**, *312*, C41. (b) Arce, A. J.; Machado, R.; De Sanctis, Y.; González, T.; Atencio, R.; Deeming, A. J. *Inorg. Chim. Acta* **2003**, *344*, 123.

(20) Mani, D.; Vahrenkamp, H. *Chem. Ber.* **1986**, *119*, 3639.

(21) Alvarez, C. M.; Alvarez, M. A.; García-Vivó, D.; García, M. E.; Ruiz, M. A.; Sáez, D.; Falvello, L. R.; Soler, T.; Herson, P. *Dalton Trans.* **2004**, 4168.

(22) For reviews on the reactivity of paramagnetic organometallic compounds see, for example: (a) In *Paramagnetic Organometallic Species in Activation Selectivity, Catalysis*; Chanon, M., Julliard, M., Poite, J. C., Eds.; Kluwer Academic Publishers: Dordrecht, 1989. (b) In *Organometallic Radical Processes*; Trogler, W. C., Ed.; Elsevier: Amsterdam, 1990. (c) Astruc, D. *Electron Transfer and Radical Processes in Transition-Metal Chemistry*; VCH: New York, 1995. (d) Sun, S.; Sweigart, D. A. *Adv. Organomet. Chem.* **1996**, *40*, 171. (e) Poli, R. *Chem. Rev.* **1996**, *96*, 2135. (f) Hoff, C. D. *Coord. Chem. Rev.* **2000**, *206*, 451. (g) Torraca, K. E.; McElwee-White, L. *Coord. Chem. Rev.* **2000**, *206*, 469. (h) Smith, K. M. *Organometallics* **2005**, *24*, 778. (i) Geiger, W. E. *Organometallics* **2007**, *26*, 5738.

(23) Brauer, D. J.; Hietkamp, S.; Sommer, H.; Stelzer, O.; Muller, G.; Kruger, C. *J. Organomet. Chem.* **1985**, *288*, 35.

(24) Neuman, M. A.; Tohan, T.; Dahl, L. F. *J. Am. Chem. Soc.* **1972**, *94*, 3383.

(25) Wadepohl, H.; Gebert, S.; Pritzkow, H. *J. Organomet. Chem.* **2000**, *614*, 158.

(26) Yeh, W.-Y.; Liu, Y.-C.; Peng, S.-M.; Lee, G.-H. *J. Organomet. Chem.* **2004**, *689*, 1014.

(27) (a) Colbran, S. B.; Johnson, B. F. G.; Lewis, J.; Sorrell, R. M. *J. Organomet. Chem.* **1985**, *296*, C1. (b) Deeming, A. J.; Doherty, S.; Day, M. W.; Hardcastle, K. I.; Minassian, H. *J. Chem. Soc., Dalton Trans.* **1991**, 1273.

(28) Haupt, H. J.; Schwefer, M.; Egold, H.; Flörke, U. *Inorg. Chem.* **1995**, *34*, 5461.

(29) Armarego, W. L. F.; Chai, C. *Purification of Laboratory Chemicals*, 5th ed.; Butterworth-Heinemann: Oxford, U.K., 2003.

(30) Labinger, J. A.; Madhavan, S. *J. Organomet. Chem.* **1977**, *134*, 381.
(31) *Collect*; Nonius BV: Delft, The Netherlands, 1997−2004.
(32) Otwinowski, Z.; Minor, W. *Methods Enzymol.* **1997**, *276*, 307.
(33) Blessing, R. H. *Acta Crystallogr., Sect. A* **1995**, *51*, 33.
(34) Farrugia, L. J. *J. Appl. Crystallogr.* **1999**, *32*, 837.
(35) Sheldrick, G. M. *Acta Crystallogr., Sect. A* **2008**, *64*, 112.
(36) *APEX* 2, version 2.0-1; Bruker AXS Inc.: Madison, WI, 2005.
(37) *SMART & SAINT Software Reference Manuals*, version 5.051 (Windows NT version); Bruker Analytical X-ray Instruments: Madison, WI, 1998.
(38) Sheldrick, G. M. *SADABS, Program for Empirical Absorption Correction*; University of Göttingen: Göttingen, Germany, 1996.